OBSERVATIONS OF SOLAR GAMMA RAY CONTINUUM BETWEEN 360 keV AND 7 MeV ON AUGUST 4, 1972*

A. N. SURI, E. L. CHUPP, D. J. FORREST, and C. REPPIN**
Dept. of Physics, University of New Hampshire, Durham, N.H. 03824

(Received 25 September, 1974; in revised form 8 April, 1975)

Abstract. Measurements were made of the time-averaged gamma ray energy loss spectrum in the energy range 360 keV to 7 MeV by the gamma ray detector on the OSO-7 satellite during the 3B flare on August 4, 1972. The differential photon spectrum unfolded from this spectrum after subtracting the background spectrum and contributions from gamma ray lines is best described by a power law with spectral index of 3.4 ± 0.3 between 360–700 keV and by an exponential law of the form $\exp(-E/E_0)$ with $E_0 = 1.0 \pm 0.1$ MeV above 700 keV. It is suggested that this spectrum is due to non-thermal electron bremsstrahlung from a population of electrons, with a strong break in the spectrum at 2 MeV. Since the observational data indicates that the matter number density must be $n_H \geq 5 \times 10^{10}$ cm^{-3} in the production region, the number of electrons above 100 keV required to explain the results is $\leq 2 \times 10^{34}$.

1. Introduction

In order to understand the mechanism(s) by which electrons and protons are accelerated to high energies in solar flares, it is essential to study the characteristics of the various emissions produced by these energetic particles. The August 1972 series of solar flares provided fairly detailed data on the impulsive X-ray, gamma ray, and radio emissions, and also on flare associated charged particles in space. In this paper we discuss the characteristics of the continuum energetic photon spectrum >360 keV observed during the August 4, 1972 3B flare. First, we briefly summarize the spectral characteristics of impulsive hard X-ray bursts and their correlation with the impulsive radio emission as observed in the past.

Impulsive solar X-ray bursts with energies ≤ 200 keV have been studied extensively over the past few years (Kane and Anderson, 1970; Kane, 1973; Frost and Dennis, 1971; Brini *et al.*, 1973; Van Beek, 1973; and Peterson *et al.*, 1973). In the energy range 10–200 keV the differential photon spectrum is usually a power law of the form $kE^{-\gamma}$ with $\gamma = 2.3$–5. However, only a few measurements extending into the gamma ray continuum >200 keV have been made in the past. Peterson and Winckler (1959) observed an energetic burst in close time coincidence with radio burst and the sudden brightening of Hα in a Class 2 flare on March 20, 1958. Though no detailed spectral measurements were possible with the Geiger counters and ionization chambers used, the authors concluded, based on a study of the relative response of the two instruments, that the spectrum extended beyond 500 keV. Observations of Cline *et al.* (1968)

* This work was supported by NASA.
** Permanent address, Max-Planck Institute for Extraterrestrial Physics, 8046 Garching by Munich, F.R.G.

Solar Physics **43** (1975) 415–429.

made during the 3B optical flare of July 7, 1966 with a scintillation counter, showed the spectral shape of this event to be consistent with a power law differential spectrum with $\gamma \approx 4.2$ in the energy range 80–400 keV. Gruber *et al.* (1973) measured the gamma ray continuum extending to ~ 6 MeV associated with the 3B optical flare of May 23, 1967 with a scintillation counter. Their measurements had sufficient spectral sensitivity to show a break in the slope of the differential photon spectrum at ~ 600 keV with a spectral index, $\gamma = 3.2$ between 25–600 keV and $\gamma = 1.2$ above 600 keV.

Several authors (e.g. Kundu, 1961; Cline *et al.*, 1968; Frost, 1969) have pointed out that excellent temporal correlation exists between the impulsive hard X-ray and microwave radio bursts. This strong correlation has been interpreted to suggest that these two different types of emissions are produced by the same population of energetic electrons (cf. e.g. De Feiter, 1974).

The purpose of this paper is to present the gamma ray continuum observations made in the energy interval 0.36–7 MeV during the 3B optical flare of August 4, 1972 and to describe the unfolded continuum high energy photon spectrum, the average electron spectrum that can be deduced from this photon spectrum; and to show the approximate time correlation of the energetic photons with photons < 100 keV and with the radio bursts. Observations of the gamma ray line emission associated with this event have been previously reported by Chupp *et al.* (1973).

2. Observations

The gamma ray detector on the OSO-7 satellite has been described in detail by Higbie *et al.* (1972). Briefly, the detector consisted of a 7.6 cm × 7.6 cm Na I (Tl) crystal surrounded by a cup-shaped active shield of Cs I (Na) and was located in the spinning wheel section of the spacecraft. Two pulse height spectra were accumulated simultaneously over nearly 3 min (90 wheel rotations) in the solar and the antisolar (i.e., background) quadrants using a 377-channel quadratic pulse height analyzer. The pulse height spectra in the energy range 0.3 to 9 MeV was calibrated twice each orbit at day/night and night/day transitions. An auxiliary X-ray detector was also included in the instrument; however, this detector suffered saturation and pulse pile up problems during most of the August 4 event.

The August 4, 1972 event began in Hα at 0617 UT, reached maximum at $\sim$0640 UT and ended at $\sim$0852 UT (Leighton and Lincoln, 1973). When the satellite emerged into daylight before the flare at $\sim$0541 UT, the rates in our lowest X-ray channels were higher by factors of ~ 70 over their average nonflare values indicating that the preflare thermal X-ray brightening had already begun. At about 0610 UT, another increase was observed, followed by the major rise at $\sim$0619 UT. Dere *et al.* (1973) report that the main event began at $\sim$0610 UT in their 4–25 keV detector. Before the OSO-7 spacecraft went into eclipse at 0633.6 UT, excess gamma ray line and continuum emission was observed. The intensity time profiles of the event after 0615 UT in the gamma ray continuum (0.36–7 MeV) and $\gtrsim 100$ keV X-rays (taken from the front shield of the OSO-7 instrument) are shown in Figure 1. These readings were

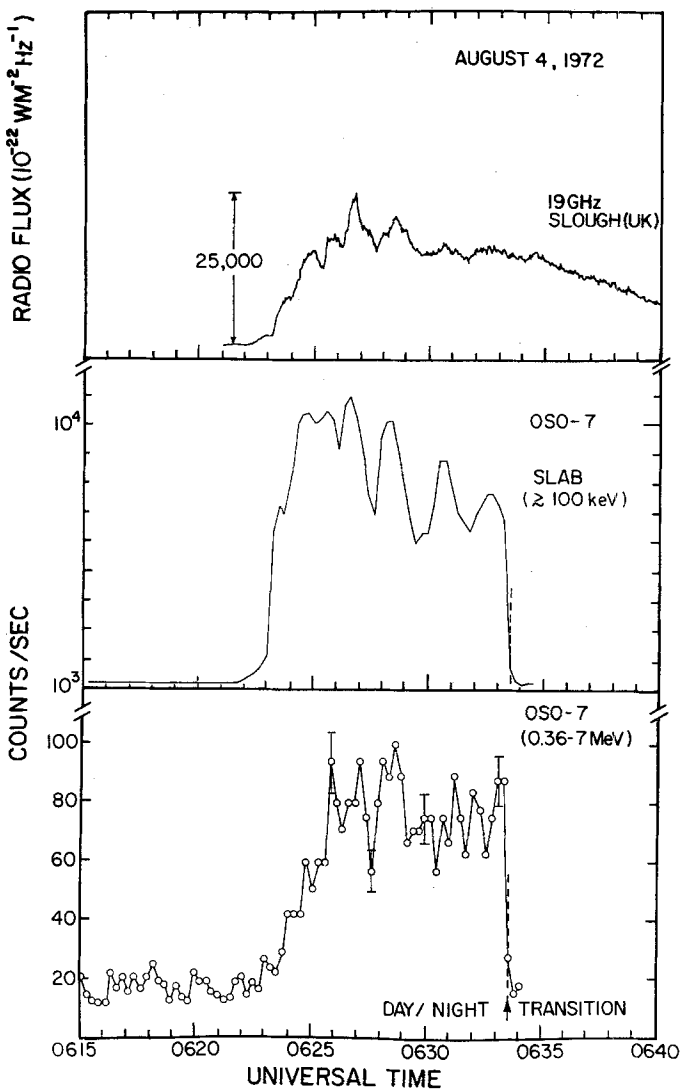

Fig. 1. The time history of the total gamma ray counting rate in the energy range 0.36–7 MeV and of the front shield ($\gtrsim$ 100 keV) as recorded by a rate meter with 15 s time resolution is shown. Also shown in this figure is the time profile of the radio burst at 19 GHz recorded at Slough (U.K.).

taken from counting rate meters, which were sampled once every 15 s. The impulsive radio burst recorded at Slough, U. K., at 19 GHz (Croom and Harris, 1973) is also shown in this figure. As can be seen there is good time correlation between these three bands and in particular, note the presence of impulsive spikes of $\sim$1 min duration. Although these spikes are not well defined in the gamma ray continuum data because of statistical limitations, the correlation between the X-ray data ($>$100 keV)

and the radio burst data is very good. The impulsive spikes in the August 4 flare have also been reported by Van Beek (1973) with much better time resolution. These latter measurements were made with the University of Utrecht hard X-ray detector on TD-1A which has a time resolution of 1.2 s (<100 keV) and 4.8 s (>100 keV). These data show that the hard X- and γ-ray consisted of several impulsive spikes with rise and decay times of 20–40 s and of duration of $\sim$1 min. The position of the 1 min spikes in the X-ray and radio data (See Figure 1 and Van Beek, 1973) agree to within 30 s in absolute time, which is near the limit of the timing accuracy that can be expected, considering the different time response of the instruments.

There is further evidence that X-ray emission occurs in shorter duration bursts, as observed in smaller flares by Van Beek *et al.* (1974). These phenomena consist of a succession of short-lived spikes (1–2 s) in the hard X-ray intensity (>24 keV) during the impulsive phase of small flares and are believed to reflect the time variation of the

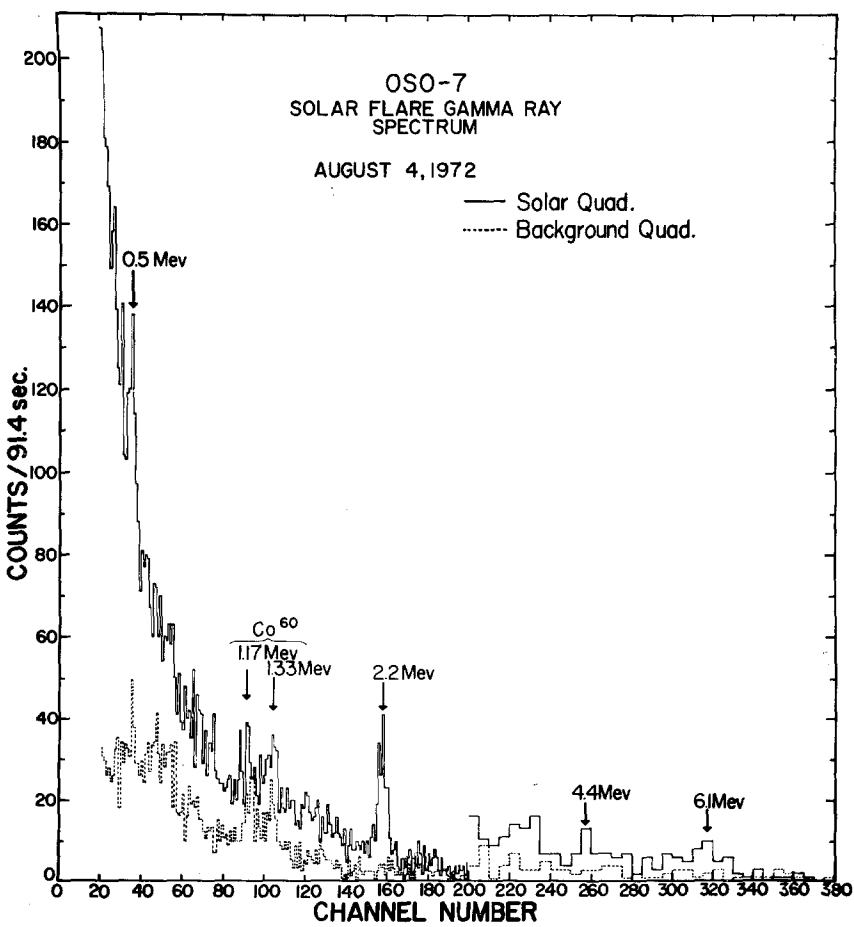

Fig. 2. The time integrated gamma ray spectrum in the solar and background quadrants accumulated during the time period 0624 to 0633 UT.

ejection of energetic electrons. The authors (Van Beek *et al.*, 1974) consider these short bursts to be the essential physical phenomena which when clustered together in large numbers, as may be the case in the August 4 flare, constitute the conventional high energy flare.

Figure 2 shows the time-integrated solar and background gamma ray pulse height spectra accumulated between 0624–0633 UT. These spectra show the total number of counts accumulated in each channel, up to channel 200, and the sum of the counts in five consecutive channels thereafter. There is significant enhancement of the counting rate extending up to 7 MeV in the solar quadrant. In addition to continuum emission, line emission at 0.5 and 2.2 MeV is clearly evident and statistically significant spectral features at 1.6, 4.4, and 6.1 MeV, are also present (Chupp *et al.*, 1973). The Co^{60} lines at 1.17 and 1.33 MeV are from the on-board calibration source.

3. Deduction of Continuum Photon Spectrum

The differential photon spectrum unfolded from the gamma ray pulse height data averaged over the time 0624–0633 UT is shown in Figure 3. Since the OSO-7 X-ray detector saturated during the impulsive phase, we also show the spectrum observed at lower energies with the X-ray detector on TD-1A which did not saturate or suffer pulse pile up limitations during the August 4 event (Van Beek, 1973). The spectrum above 360 keV in Figure 3 was obtained by first subtracting the background quadrant counting rate spectrum from the solar quadrant counting rate spectrum. Next, the photopeak and Compton continuum contributions from gamma ray lines at 0.5, 1.6, 2.2, 4.4, and 6.1 MeV were subtracted. The solar photon spectrum incident on the detector was found by transforming this counting rate spectrum, through the detector response, by the 'strip-off' method (Burrus, 1960).

The first step in this procedure consisted of obtaining a reasonably accurate measure of the Compton continuum and of the first and second escape peaks for various energies of interest for the detector. Calibration response function data collected with the OSO-7 detector by Higbie *et al.* (1973) was used for this purpose. Correction for these effects is of lesser importance with the OSO-7 detector than with an unshielded detector since the anticoincidence action of the Cs I shield reduces the Compton continuum and escape peaks by a factor of ~ 2.4. The energy range 0.36–7 MeV (no excess counts were observed above 7 MeV) was then divided into 25 energy bins of widths varying from 0.1 MeV at the low energy end to 0.5 MeV at the high energy end. Starting with the highest energy bin, the contribution of the Compton continuum and escape peaks associated with the counts in this bin was subtracted from all the lower energy bins. This procedure was repeated with the second highest bin and so on down to the last bin at 0.37 MeV. This correction was less than 20% of the observed counting rates below 0.7 MeV. However, at higher energies, where the spectrum becomes harder, the correction was about 30%, 50%, 44%, 33%, and 11% for the energy bins 1–2, 2–4, 4–5, 5–6, and 6–6.5 MeV, respectively.

The incident photon spectrum can now be calculated from this 'Compton-corrected'

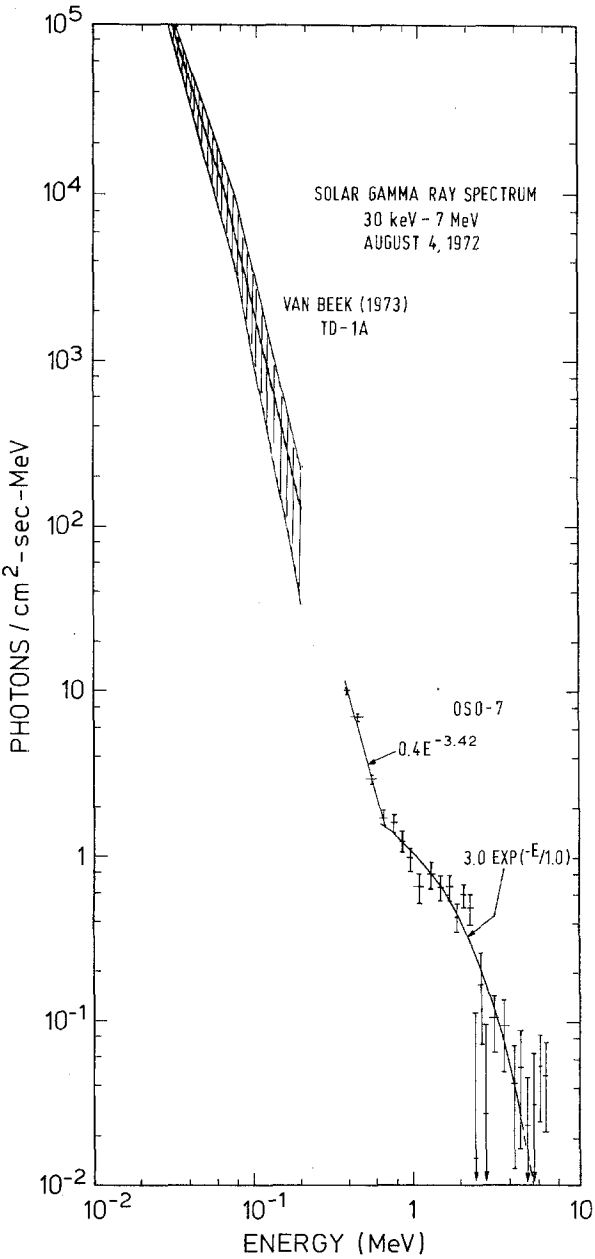

Fig. 3. The differential gamma ray continuum spectrum observed during the time interval 0624–0633 UT and the hard X-ray spectrum observed from TD-1A. The solid line represents the average spectral shape averaged over eight time intervals between 0623.5–0630.5 UT as given by Van Beek (1973).

counting rate spectrum by dividing the remaining counting rates in each channel by the energy dependent photopeak sensitivity. The photopeak sensitivity up to 3 MeV was obtained by Higbie *et al.* (1973) for the OSO-7 detector. Above 3 MeV results of Monte Carlo calculations by Giannini *et al.* (1970), for a parallel beam incident on a $3'' \times 3''$ Na I crystal were used. The final result of these calculations is the incident photon spectrum shown in Figure 3.

The differential photon spectrum in the energy range 360–700 keV was fit to a power law by a least square method with the result that

$$dJ/dE = 0.4\, E^{-3.4\pm0.3} \text{ photon cm}^{-2}\text{ s}^{-1}\text{ MeV}^{-1}. \quad (1)$$

Although a power law fit to the spectrum in the range 0.7–7 MeV cannot be entirely ruled out, an exponential of the form,

$$dJ/dE = 3.0 \exp(-E/E_0) \text{ photon cm}^{-2}\text{ s}^{-1}\text{ MeV}^{-1}, \quad (2)$$

where $E_0 = (1.0 \pm 0.1)$ MeV gives a better fit. The value of the reduced χ^2 for this fit was 1.7 for 19 deg of freedom. A power law fit to the data above 700 keV gives $dJ/dE = 1.0\, E^{-1.7}$ photon cm^{-2} s^{-1} MeV^{-1}, with a reduced $\chi^2 = 2.3$ for 19 deg of freedom. However, we do not observe any excess counts between 7 and 8 MeV above the expected 5 background counts while we expect 6 excess counts if the power law given above represents the data. This again indicates that the data above 700 keV is best described by an exponential rather than a power law.

The derived average photon power law spectrum in the energy range 360–700 keV is consistent in both intensity and spectral shape with the photon spectrum observed in the energy range 29–203 keV on TD-1A. Van Beek (1973) selected eight time intervals during the period 0623.5–0630.5 UT and determined parameters k and γ of the photon spectrum below and above the low energy break in the photon spectrum at $\approx$90–100 keV. The spectral index varied between 2.7 and 3.5 below the break and between 3.5 and 5.1 above the break. This is shown by the hatched area in Figure 3. The solid line in the hatched area represents the spectral slope averaged over the eight time intervals.

Since it is clear that a single power law spectrum describes the data from $\sim$100 to $\sim$700 keV, it is important to evaluate possible causes of the abrupt change in the spectrum at $\sim$700 keV.

4. Shape of the Continuum Spectrum above 700 keV

We have considered the following effects which could give rise to the flattening of the gamma ray continuum: Compton scattering of the 2.23 MeV neutron capture photons in the solar photosphere, Compton scattering of the same gamma ray line in the Earth's atmosphere, and possible direct or indirect effects from energetic nucleons in the solar atmosphere.

Ramaty and Lingenfelter (1973) and Reppin *et al.* (1973) have investigated the fate of energetic neutrons produced on the Sun and have shown that most of the downward moving neutrons are slowed down and captured at a columnar depth of 2–4 g cm^{-2} in the photosphere where they produce 2.23 MeV photons by capture on hydrogen. Wang and Ramaty (1974) and Kanbach (Kanbach, private communication, 1975) have carried out Monte Carlo calculations on the transport of these 2.23 MeV photons out of the photosphere and find that $\lesssim 20\%$ of the observed flux at 2.23 MeV would be Compton scattered into the energy region 1–2 MeV. Since the observed continuum flux between 1–2 MeV is 0.7 $cm^{-2}\,s^{-1}$ and the 2.23 MeV flux is 0.28 $cm^{-2}\,s^{-1}$, it does not appear that this effect can account for the flattening of the spectrum above 700 keV.

Because of the broad angular response of the gamma ray detector ($\sim 100°$), it is likely that the instrument registered atmospheric scattered radiation during a portion of the event just prior to the day/night transition. A detailed treatment of the problem is complex; however, it is possible to give an estimate of this effect by using the Monte Carlo calculations of gamma ray scattering carried out by Berger and Raso (1960). Since the effective Z of air is close to that of water, we have used their results for scattering of 2 MeV gamma rays from water. Considering the worst case of grazing incidence, we estimate from their results that the flux of atmosphere scattered 2.23 MeV photons in the energy range 0.7–2 MeV can only be $\sim 6\%$ of the observed continuum.

Another possibility to be considered is that the spectrum >700 keV is due to direct or indirect nucleon processes at the Sun. Hudson (1973) has considered direct proton bremsstrahlung for the August 4 flare and found that this falls more than six orders of magnitude below the observed gamma ray spectrum. It is possible however that the observed spectrum is due to bremsstrahlung from the decay electrons and positrons of the π mesons produced in nuclear reactions. The flux of the 0.51 MeV line (6.3×10^{-2} photon $cm^{-2}\,s^{-1}$) observed during the August 4 event implies that the rate of annihilation of positrons at the Sun was $\sim 1.3 \times 10^{26}\ s^{-1}$. If we assume that all the positrons annihilating were from π^+ mesons, then under quasi-equilibrium conditions, $\sim 2.6 \times 10^{26}\ s^{-1}$ must also be the slowing down rate of fast electrons and positrons ($\sim$20–50 MeV) resulting from the decay of π^- and π^+ mesons. These electrons and positrons will lose most of their energy as a result of synchrotron radiation and ionization loss. Taking the ratio of radiation loss (bremsstrahlung) to the total energy loss to be $\sim 10^{-4}$ (Cheng, 1972), the radiation energy is $\sim 4 \times 10^{18}$ erg s^{-1}, which is about four orders of magnitude smaller than the $\sim 10^{22}$ erg s^{-1} observed in the gamma radiation >700 keV.

There still exists the possibility that a part of the observed flux >700 keV is due to a large number of unresolved gamma ray lines. Ramaty *et al.* (1975) have calculated the fluxes of various prompt gamma ray lines produced during solar flares. Scaling the intensity of these unresolved lines to the observed line at 4.43 MeV from $^{12}C^*$ (3×10^{-2} photon $cm^{-2}\,s^{-1}$), we estimate that the contribution from these unresolved lines is about 3% of the observed flux in the energy range 0.7–3 MeV. Thus the shape

of the continuum spectrum above 700 keV cannot be due to predicted, but unresolved gamma ray lines. Furthermore, the energy resolution of the OSO-7 detector for a single gamma ray line is ~ 5 channels and the energy range 0.7–3 MeV covers approximately 120 channels. Therefore, about 25 unpredicted gamma ray lines all at nearly the same intensity would be required to produce the observed flattening of the spectrum.

We conclude that the change in spectral shape at ~ 700 keV is real and not an artifice of either local atmospheric or any obvious proton effects, and that it must be produced by bremsstrahlung from a hard nonthermal spectrum of electrons at the Sun.

5. Discussion

In the following, we will relate the observed gamma ray continuum spectrum to the characteristics of the energetic electrons in the flare region. The observations show the photon continuum is best fit by a power law below 700 keV and an exponential above 700 keV. If we assume that the power law spectrum extends beyond 700 keV, then the difference between the observed and the power law spectrum yields a difference photon spectrum that is zero at ~ 700 keV, reaches a maximum at ~ 1.5 MeV and then falls off exponentially. Since it is impossible to produce such a spectrum from electron bremsstrahlung, we conclude that these observations strongly suggest that the X- and γ-ray flux is produced by a single population of electrons with a break in its spectrum and not by two separate populations of electrons acting independently. If this conclusion is confirmed by future experiments with higher time resolution at high energies, it will provide an important constraint on the electron acceleration mechanisms.

The most readily available theoretical calculations using relativistic cross sections for electron-proton bremsstrahlung in the solar atmosphere are those of Holt and Cline (1968) and Cheng (1972). (See also De Feiter (1974) for a review of these calculations.) Cheng (1972) has calculated the expected flux of continuum gamma radiation at the Earth from solar flares assuming a power law in energy, as well as an exponential in rigidity electron distributions. These calculations show that electron-proton bremsstrahlung from a power law electron spectrum produces a photon spectrum which is also a power law to a good approximation. An exponential rigidity electron spectrum produces a photon spectrum which cannot be simply expressed analytically but is similar to an exponential shape. Since a power law differential photon spectrum is observed between 360 and 700 keV, we assume that the instantaneous spectrum of accelerated electrons is a power law of the form (Cheng, 1972; Holt and Cline, 1968),

$$n(\gamma_e) = A(\gamma_e - 1)^{-\alpha}, \tag{3}$$

where A is a constant having the dimensions of number density per unit electron Lorentz factor, $(\gamma_e = E/m_0c^2 + 1)$, and α is the electrons spectral index. At higher energies an exponential electron spectrum of the form

$$n(R) = A' \exp(-R/R_0) \tag{4}$$

is assumed, where R is the rigidity of the electron and R_0 is the characteristic rigidity and A' has the dimensions of number density per unit electron rigidity measured in units of m_0c^2 per electron charge. For a power law electron spectrum given by Equation (3) or an exponential spectrum given by Equation (4) the expected flux of gamma radiation at the Earth is given by (Cheng, 1972)

$$I(E_\gamma) = 5.68 \times 10^{-44} E^{-1}_{\gamma\,(\mathrm{MeV})} EM q(E_\gamma) \text{ photon cm}^{-2}\text{ s}^{-1}\text{ MeV}^{-1}, \quad (5)$$

where $q(E_\gamma)$ is the source strength of emitted photons and $EM = An_H V$, is the emission measure in units of particles cm^{-3}. Here n_H is the ambient proton density and V is the volume. For a power law electron spectrum,

$$q(E_\gamma) = f(\alpha)\, E^{-\alpha+1}_{\gamma\,(\mathrm{MeV})} \quad (6)$$

and is shown in Figure 3.13 of the Cheng (1972) paper plotted for several values of α.

The calculated gamma ray continuum spectrum fits the observed spectrum between 360 and 700 keV for $\alpha = 3.4$ and for $EM = 5.3 \times 10^{43}$ cm^{-3}.

For the exponential spectrum, Cheng gives plots of the source strength $q(E_\gamma)$ for different values of R_0 in his Figure 3.14. The calculated fluxes obtained by substituting $q(E_\gamma)$ corresponding to $R_0 \simeq 5$ MV and $EM = 6.5 \times 10^{41}$ cm^{-3} fit the observation above 700 keV.

To find the electron spectrum in the source region from these results we note that

$$n(E) = n(\gamma)\frac{d\gamma}{dE} = A(\gamma_e - 1)^{-\alpha}\frac{1}{m_0c^2}$$

for the power law, and

$$n(E) = n(R)\frac{dR}{dE} = A'\frac{\gamma_e}{m_0c^2\sqrt{(\gamma_e^2 - 1)}}\exp[-0.511(\gamma_e^2 - 1)^{1/2}/R_0]$$

for the exponential rigidity spectrum.

Making the appropriate substitutions, multiplying by the volume V and noting at $AV = EM/n_H$, we have for the power law electron spectrum

$$N(E) = \frac{1.1 \times 10^{43}}{n_H} E^{-3.4}_{(\mathrm{MeV})} \text{ electron MeV}^{-1} \quad (7)$$

and for the exponential rigidity electron spectrum

$$N(E) = \frac{1.3 \times 10^{42}}{n_H}\frac{\gamma_e}{\sqrt{(\gamma_e^2 - 1)}} \times \exp[-0.511(\gamma_e^2 - 1)^{1/2}/R_0] \text{ electron MeV}^{-1}, \quad (8)$$

where $E = 0.511(\gamma_e - 1)$ is the kinetic energy of the electron in MeV, n_H is in number per cm^3, and R_0 is 5 MV. The final source spectrum of electrons as given by these two equations is shown in Figure 4. This spectrum represent the electron distribution

for the total number of flare electrons that is *sufficient* to produce the observed X- and gamma ray time-averaged spectrum if it was produced by bremsstrahlung in a thin target production model (i.e. $dN(E)/dt \approx 0$ over the observing period). Since the observed radiation may be produced in a thick target (i.e. $dN(E)/dt \neq 0$ over the observing period), the original spectrum of electrons introduced into the source region may be quite different from the 'averaged' spectrum derived here and shown in Figure 4.

In order to determine the actual number of electrons involved in the emission, the density of the source region (n_H) must be known. Time structure in the X-ray emission of less than 1 s has led Van Beek *et al.* (1974) to estimate the ambient electron density

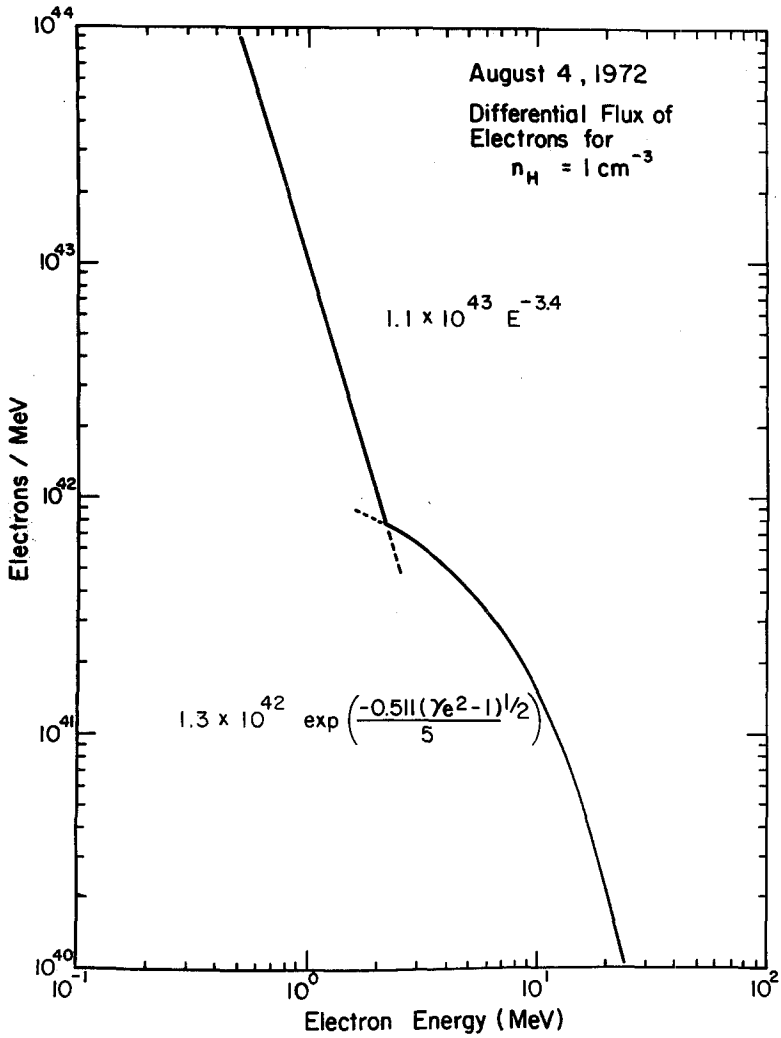

Fig. 4. Instantaneous time averaged electron spectrum derived from the observed photon spectrum shown in Figure 3.

in the X-ray source region to be $\geqslant 5\times 10^{10}$ cm^{-3} and the time history of the 0.511 MeV annihilation gamma ray line observed during this event (Chupp *et al.*, 1975) shows that the annihilation takes place in a region where the ambient electron density is at least as high as the value given above. Using $n_H \geqslant 5\times 10^{10}$ cm^{-3}, the total number of electrons $\geqslant 0.1$ MeV from Equation (7) is

$$N(>0.1 \text{ MeV}) \leqslant \frac{1.1\times 10^{43}}{5\times 10^{10}} \int_{0.1}^{\infty} E^{-3.4}\, dE \leqslant 2.3\times 10^{34}.$$

The number of electrons contributed by the exponential shape given by Equation (8) is only significant for electrons above 2 MeV. We also note that very similar electron spectra for the August 4 flare was independently obtained by Ramaty *et al.* (1975).

It was pointed out in Section 2 that there was very good time correlation between the impulsive hard X-ray and microwave bursts in this event. This striking temporal correlation indicates that both types of emissions are produced by the same population of electrons. It is therefore of interest to derive the spectral index (α') and the total number of nonthermal electrons responsible for the radio burst and compare these with those derived from the hard X-rays.

The frequency at which the observed microwave flux is a maximum [f_{max} (MHz)] is related to the gyro-frequency [f_H (MHz)] and the magnetic field strength in the source region [B (gauss)] by the relation $f_{max} \approx 3.5 f_H \approx 9.8\, B$ (Takakura, 1967). For the August 4 event, $f_{max} \approx 15$ GHz (Croom and Harris, 1973). Therefore, $B \approx 15000/9.8 \approx 1530$ G. At frequencies above f_{max} the microwave burst flux is approximately proportional to $f^{(1-\alpha')/2}$ (Takakura and Scalise, 1970), where α' is the spectral index of the relativistic electron power law spectrum. Above f_{max} the radio spectrum was a power law with a spectral index ≈ -1 up to 37 GHz and flattens above 37 GHz (Croom and Harris, 1973). Therefore, $(1-\alpha')/2 \approx -1$ or $\alpha' \approx 3$, which is in general agreement with the gamma ray continuum data <700 keV. The flattening of the radio power spectrum above 37 GHz perhaps reflect the change in the shape of the electron distribution above 2 MeV. However, this cannot be confirmed since the highest frequency at which the solar radio burst was recorded was 71 GHz. Radio data above 100 GHz will be needed to get a clear idea of the shape of the higher energy electron spectrum producing the higher frequencies.

To estimate the total number of electrons responsible for the microwave emission, we have used the model proposed by Takakura (1972). This model assumes a nonuniform magnetic field in the radio source region and takes into account self-absorption. The source region is set at the base of the corona with an average density of $\sim 5\times 10^9$ cm^{-3}. The magnetic field strength in the source region is nonuniform and depends on the assumed magnetic field strength at the photosphere. Takakura assumed a magnetic field strength of 2500 G at the photosphere and this gives a maximum value in the source region of ~ 1175 G. By comparing the observed radio spectrum of Croom and Harris (1973) averaged over the time interval 0624–0633 UT with the theoretical spectrum calculated by Takakura (1972) (see Figure 2 of Takakura's paper

where $B(0)=2500$ G, $\mathrm{d}/\mathrm{d}S=1.4$ and $\xi=\sqrt{3}$), we find that the total number of electrons above 100 keV is about 2×10^{35} which is about 10 times larger than is needed to produce the X- and γ-ray emission. It may be that a small change in some of the parameters in Takakura's model can resolve this discrepancy.

The observation of electrons and protons in interplanetary space can provide a direct sample of the accelerated particles produced in solar flares. The observations of nonrelativistic and relativistic electrons associated with the August 4 event have been made by Lin and Anderson (1973) and Domingo *et al.* (1973), but spectral information is not yet available. The observations of gamma ray line emission in coincidence with the X- and γ-ray continuum during this event suggest that electrons and protons were essentially accelerated simultaneously. Forrest *et al.* (1975) have investigated the production of gamma ray lines and the isotopes of deuterium and ^{3}He observed during this event (Webber *et al.*, 1975). Assuming that the isotopes were produced during the impulsive phase when the gamma ray lines were observed, they found that the density in the source region must be $n_{\mathrm{H}}\gtrsim2\times10^{10}$ cm^{-3} depending on the particle containment time.

It is clear that a consistent interpretation of the hard X-ray, microwave and nuclear secondary emissions, observed during the August 4 event suggests a density of $\geqslant10^{10}$ cm^{-3} in the acceleration region.

6. Summary

This paper presents the first measurements of the solar flare gamma ray continuum extending up to ~7 MeV with good energy resolution. We have shown that this continuum is due to energetic electrons and that any effects from protons such as unresolved lines are negligible. The differential photon spectrum is best described by a power law between ~100 keV and ~700 keV and by an exponential shape above 700 keV. The average photon spectrum can be explained by a single *time-averaged* population of electrons with a sudden hardening of the spectrum at ~2 MeV. A similar spectral hardening has been observed in another large flare and may be a characteristic of the acceleration process.

The relativistic bremsstrahlung calculations discussed here indicate that the total number of electrons greater than 100 keV, required to produce the observed X- and gamma ray continuum, is $\lesssim2\times10^{34}$. This was determined from the observational requirement that the ambient matter number density in the production region must be $n_{\mathrm{H}}\geqslant5\times10^{10}$ cm^{-3}. The close similarity in the intensity-time profiles of the impulsive radio and gamma ray continuum suggests that the two types of emissions are due to synchrotron radiation and bremsstrahlung respectively from the same population of nonthermal electrons. The observations indicate that a major fraction of both the X-ray and radio emissions occur in bursts with durations less than 1 min. There is some evidence from other experiments that the fundamental emissions occur in bursts that are less than 1 s in duration.

It is clear that further understanding of these flare phenomena requires more obser-

vations of the high energy photon continuum with instruments that have time resolutions of less than 1 s, higher sensitivity, and good energy resolution beyond MeV photon energies. In addition it should be emphasized that simultaneous spectral measurements of electrons and protons in interplanetary space are also essential as these measurements provide a direct sample of the particles accelerated during solar flares.

Acknowledgements

We are grateful to Dr D. Croom for providing the radio burst data. This work was supported by NASA under contracts NGR 30-002-104 and NGL 30-002-021.

References

Berger, M. J. and Raso, D. J.: 1960, *Radiation Res.* **12**, 20; NBS Report 5982.
Brini, D., Evangelisti, F., Fuligni Di Grande, M. T., Pizzichini, G., Spizzichino, A., and Vespignani, G. R.: 1973, *Astron. Astrophys.* **25**, 17.
Burrus, W. R.: 1960, *IRE Trans. Nucl. Sci.* **NS-7**, 102.
Cheng, C. C.: 1972, *Space Sci. Rev.* **13**, 3.
Chupp, E. L., Forrest, D. J., Higbie, P. R., Suri, A. N., Tsai, C., and Dunphy, P. P.: 1973, *Nature* **241**, 333.
Chupp, E. L., Forrest, D. J., and Suri, A. N.: 1975, in S. R. Kane (ed.), 'Solar Gamma-, X-, and EUV Radiation', *IAU Symp.* **68**, 341.
Cline, T. L., Holt, S. S., and Hones, E. W.: 1968, *J. Geophys. Res.* **73**, 434.
Croom, D. L. and Harris, L. D. J.: 1973, World Data Center A, Report UAG-28, Part 1, 210.
De Feiter, L. D.: 1974, *Space Sci. Rev.* **16**, 3.
Dere, K. P., Horan, D. M., and Kreplin, R. W.: 1973, World Data Center A, Report UAG-28, Part 2, 99.
Domingo, V., Köhn, D., Page, D. E., Taylor, R. G., and Wenzel, K. P.: 1973, World Data Center A, Report UAG-28, Part 2, 342.
Forrest, D. J., Chupp, E. L., and Suri, A. N.: 1975, *Proc. Int. Conf. on X-Rays in Space*, Calgary, Canada, 14–21 August, 1974, to be published.
Frost, K. J.: 1969, *Astrophys. J. Letters* **158**, L159.
Frost, K. J. and Dennis, B. R.: 1971, *Astrophys. J.* **165**, 655.
Giannini, M., Oliva, P. R., and Ramorino, M. C.: 1970, *Nucl. Instr. Methods* **81**, 104.
Gruber, D. E., Peterson, L. E., and Vette, J. I.: 1973, in R. Ramaty and R. G. Stone (eds.), *High Energy Phenomena on the Sun*, NASA SP-342, p. 147.
Higbie, P. R., Chupp, E. L., Forrest, D. J., and Gleske, I. U.: 1972, *IEEE Trans. Nucl. Sci.* **NS-19**, 606.
Higbie, P. R., Forrest, D. J., Gleske, I. U., and Chupp, E. L.: 1973, *Nucl. Instr. Methods* **108**, 167.
Holt, S. S. and Cline, T. L.: 1968, *Astrophys. J.* **154**, 1027.
Hudson, H. S.: 1973, in R. Ramaty and R. G. Stone (eds.), *High Energy Phenomena on the Sun*, NASA SP-342, p. 207.
Kane, S. R.: 1973, in R. Ramaty and R. G. Stone (eds.), *High Energy Phenomena on the Sun*, NASA SP-342, p. 55.
Kane, S. R. and Anderson, K. A.: 1970, *Astrophys. J.* **162**, 1003.
Kundu, M. R.: 1961, *J. Geophys. Res.* **66**, 4308.
Leighton, H. I., and Lincoln, J. V.: 1973, *Solar Geophysical Data*, No. 342, Part II, U.S. Department of Commerce, February.
Lin, R. P. and Anderson, K. A.: 1973, World Data Center A, Report UAG-28, Part 2, 334.
Peterson, L. E. and Winckler, J. R.: 1959, *J. Geophys. Res.* **64**, 697.
Peterson, L. E., Datlowe, D. W., and McKenzie, D. L.: 1973, in R. Ramaty and R. G. Stone (eds.), *High Energy Phenomena on the Sun*, NASA SP-342, p. 132.
Ramaty, R. and Lingenfelter, R. E.: 1973, *Proc. 13th Int. Cosmic Ray Conf.* Denver, **2**, 1590.

Ramaty, R., Kozlovsky, B., and Lingenfelter, R. E.: 1975, *Space Sci. Rev.*, in press.
Reppin, C., Chupp, E. L., Forrest, D. J., and Suri, A. N.: 1973, *Proc. 13th Int. Cosmic Ray Conf.*, Denver, **2**, 1577.
Takakura, T.: 1967, *Solar Phys.* **1**, 304.
Takakura, T.: 1972, *Solar Phys.* **26**, 151.
Takakura, T. and Scalise, E., Jr.: 1970, *Solar Phys.* **11**, 434.
Van Beek, H. F.: 1973, Ph.D. Thesis, University of Utrecht, Holland.
Van Beek, H. F., De Feiter, L. D., and De Jager, C.: 1974, *Space Research* **14**, Akademie-Verlag, Berlin, p. 447.
Wang, H. T. and Ramaty, R.: 1974, *Solar Phys.* **36**, 129.
Webber, W. R., Roelof, E. C., McDonald, F. B., Teegarden, B. J., and Trainor, J. H.: 1975, to be published in *Astrophys. J.*